Travelling Wave Antennas with Semitransparent Surfaces for Forming a Cutoff Pattern

D. V. Tatarnikov and I. M. Chernetsky
Topcon Positioning Systems, Moscow, Russia

Abstract— Opportunities to achieve a cutoff pattern with the travelling wave antennas of moderate size are discussed. A qualitative model in the form of a parallel plate waveguide with semitransparent endings has been evaluated. A quadrifilar helix antenna with embedded reactances with the length of about 1.5 wavelength has been built. The antenna possesses a smooth pattern in the top semi-sphere with 20 dB drop of the gain (cutoff) while crossing the local horizon. Antenna functionality in applications to positioning with the Global Navigation Satellite Systems has been tested. RMS of positioning error is shown to be of 0.65 mm provided phase noise of the system smoothed out within 1 minute span.

1. INTRODUCTION

Antennas with a cutoff pattern are of special interest to various applications, in particular, to high-precision positioning with the Global Navigation Satellite Systems (GNSS). At the best open sky sites the ground reflections, referred to as multipath, are the largest error source. The multipath error is proportional [1] to antenna down-up ratio understood as $DU(\theta^e) = F(-\theta^e)/F(\theta^e)$. Here $F(\pm\theta^e)$ is the antenna pattern reading for a certain angle θ^e above (below) the local horizon. Currently, for practical antennas the DU readings are [1, 2] about $-5\ldots-7$ dB for 10 degrees getting down to $-15\ldots-25$ dB for directions close to the zenith. This sets up the best achievable positioning precision of $1\ldots2$ cm in real time. For mm-level precision the figure of multipath suppression is 20 dB or better starting from low elevations [1, 3]. Thus, the antenna is to have a smooth pattern in top semi-sphere with a sharp drop (cutoff) while crossing the horizon. So far, a vertical array antenna exceeding 10 wavelengths has been presented in [4]. The antenna is intended as a reference for automated aircraft landing. In [5], a large impedance ground plane of 15 wavelengths in diameter is shown. With the latter, multipath error is shown to fall below the system noise resulting in 0.7 mm precision of positioning with the noise filtered out.

However, the antennas of above are substantial in the wavelength scale. The paper is to discuss opportunities and present results of realizing the cutoff pattern with antenna of moderate size. One is to note a coaxial leaky wave antenna presented in [6]. The antenna forms a dipole-type omnidirectional pattern typical for communication purposes. In what follows, in Section 2 a qualitative model of a parallel plate waveguide with the semitransparent endings is discussed. The model is to evaluate the opportunities of forming the cutoff pattern. Then, in Section 3, a quadrifilar helix antenna with embedded reactances is presented. Finally, in Section 3, the results of antenna field tests in regards to positioning are shown.

2. PARALLEL PLATE WAVEGUIDE WITH SEMITRANSPARENT WALLS

The geometry under consideration is shown at the left panel of Figure 1. Here, a parallel plate waveguide is excited by a TEM wave travelling in positive z-direction. The waveguide width a is chosen such that all the higher order modes are evanescent. The waveguide plates end up with semitransparent segments of the length h shown by thick dashed lines. Semitransparency is understood such that the boundary conditions [7]

$$\begin{aligned} \vec{E}_\tau^+ = \vec{E}_\tau^- = \vec{E}_\tau \\ \left[\vec{n}_0, \vec{H}_\tau^+ - \vec{H}_\tau^-\right] = \vec{j}_S^e = \vec{E}_\tau / Z_g \end{aligned} \tag{1}$$

hold across each of the segments. In (1), $\vec{E}(\vec{H})_\tau^{+,-}$ are the tangential components of electric and magnetic field intensities at two sides of the segment, the unit normal vector $\vec{n}_0$ points from the "$-$" surface to the "+" one (see Figure 1), $\vec{j}_S^e$ is the equivalent electric current surface density, brackets [ ] stand for the cross-product, Z_g is the parameter called grid impedance [7]. The impedance is assumed to be varying as a function of z. Thin sheet layers approximating the conditions (1) are commonly known. For applications to travelling wave antennas see [6], applications to antenna ground planes could be checked in [8].

To model the radiation of the waveguide, a standard method of moments is applied. For the purpose, a perfectly conducting insert closing the waveguide at $z = 0$ is introduced. The distance L is large enough such that two conditions hold: a) it is only the TEM wave that contributes to the field intensities inside the waveguide at $z = 0$; b) electric currents flowing at the exterior of the waveguide in the domain $z < 0$ have decayed such that the currents contribution to the radiation pattern is negligible. To compensate for the insert, an equivalent magnetic current is introduced at both two sides of the insert. The magnetic current is shown by dotted lines at the left panel of the figure. In the domain $z < 0$ the fields inside the waveguide are the incident and the reflected TEM waves only; there are no electric currents at the exterior surfaces of the waveguide in the domain as mentioned.

In the domain $z > 0$, unknown electric surface currents are introduced. The currents are shown by thin dashed lines at the right panel of Figure 1. In the insert plane $z = +0$ the electric current surface density I is related to the magnetic current amplitude U such that $I = (2V - U)/(\eta_0 a)$. Here V is the incident wave voltage, η_0 is the intrinsic impedance of free space. To ensure continuity of the electric charge, two basic functions in the form of half-triangle with amplitudes I are introduced at $x = \pm a/2$; the rest of the waveguide walls are covered by triangle basic functions with amplitudes I_n. The problem is reduced to the system of linear algebraic equations with respect to I_n with the voltage U serving as a source. Matrix elements are evaluated numerically employing representations in spectral domain similar to [8].

With the calculations, the values of Z_g at the perfectly conducting surfaces were set up to zero. The profile $Z_g(z)$ at the semitransparent portion (thick dashed lines at the right panel of

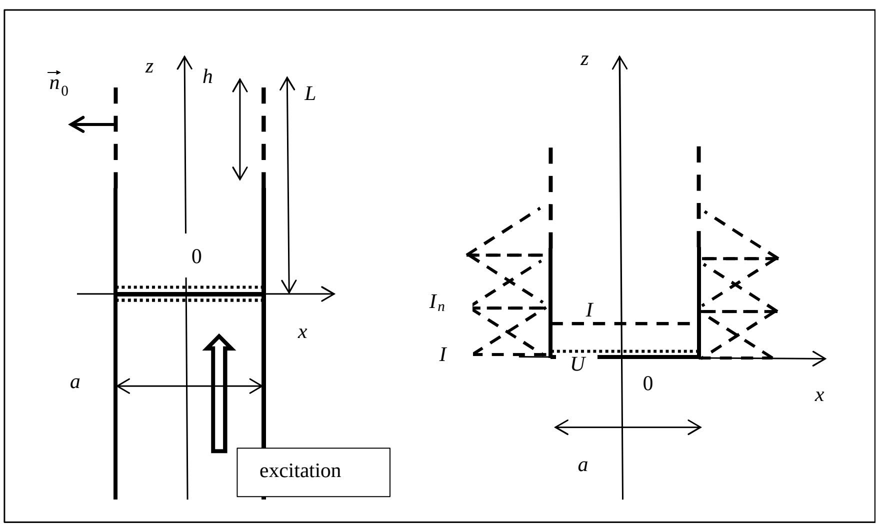

Figure 1: Geometry of the parallel plate waveguide with semitransparent endings and electric currents representation.

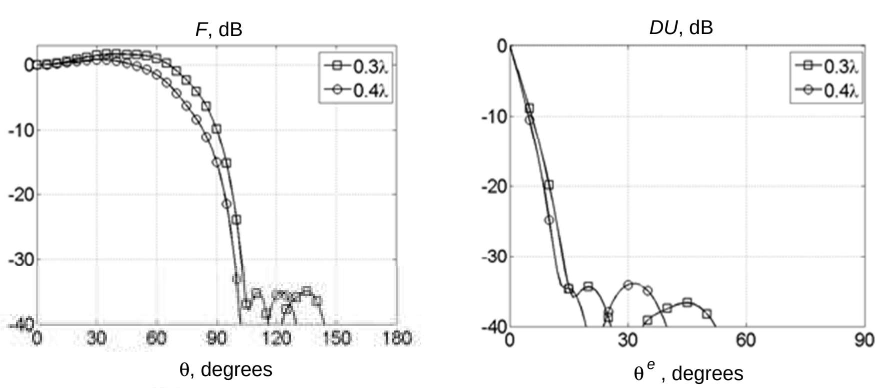

Figure 2: Calculated results for the parallel plate waveguide with semitransparent endings.

the figure) was optimized such that the cutoff radiation pattern would be achieved. The calculated results are shown at Figure 2 for the radiation pattern and down-up ratio at the left and right panels respectively. In the legend, the respective waveguide width a is shown in fractions of the wavelength. One may note that the down-up ratio exceeds 20 dB in absolute value starting from 10 degrees. It has been defined that h of about 1.5 wavelengths is sufficient. The reflection coefficient does not exceed 10^{-5} within the bandwidth of $+/-10\%$.

3. QUADRIFILAR HELIX ANTENNA WITH EMBEDDED REACTANCES

For practical implementation, a quadrifilar helix antenna with embedded reactances has been synthesized. A general view of the antenna is shown at the left image of Figure 3. Antenna is intended for L1 GNSS band (1560 ... 1610 MHz).

Measured antenna patterns for the θth and the φth linear polarized components and the down-up ratio in terms of total power are illustrated in Figure 4. As seen, antenna pattern roll-off from the zenith to 10 degrees elevation does not exceed 15 dB which is a typical practical figure for GNSS positioning antennas. The down-up ratio exceeds 20 dB in absolute value starting from 10 degrees.

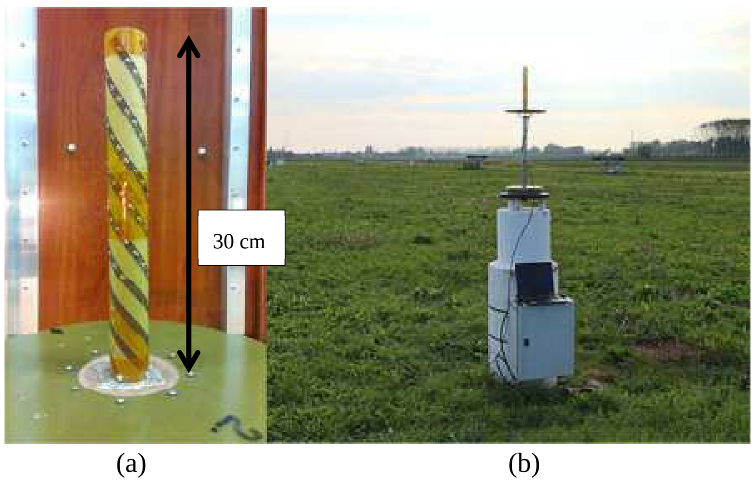

Figure 3: (a) General view of the helix antenna and (b) antenna installed at the test range.

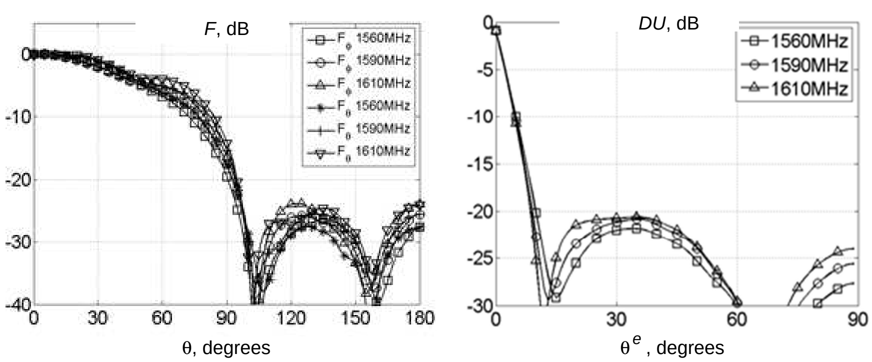

Figure 4: Measured antenna pattern for the helix antenna with embedded components and the down-up ratio.

4. FIELD TEST RESULTS

The antenna installed at the concrete pier of the test range is illustrated at the right panel of Figure 3. With differential positioning, the reference station antenna was of the same type. Real time error of positioning in the vertical coordinate is shown in Figure 5. For this data, the system noise has been smoothed within 1 minute time interval. As seen, the remaining error does not exceed $+/-1.7$ mm with RMS estimated as 0.65 mm. The result coincides with that reported in [5].

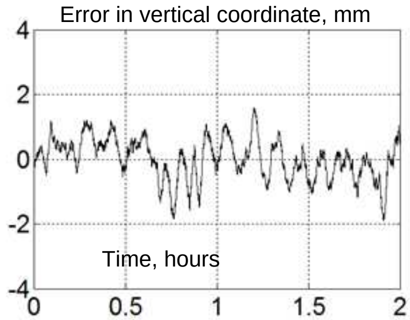

Figure 5: Real time error in vertical coordinate with the noise smoothed out within 1 minute span.

5. CONCLUSION

The results presented indicate that the cutoff pattern with about 20 dB drop of the gain while crossing the local horizon is achievable with travelling wave antennas of about 1.5 wavelengths size. With this kind of the pattern, it is no longer multipath but rather the system noise that is the largest error source in satellite positioning. Rms of positioning below 1 mm after smoothing the noise within about 1 minute span is shown. Thus, such kind of positioning in "almost" real time may become of practical interest.

REFERENCES

1. Leick, A., L. Rapoport, and D. Tatarnikov, *GPS Satellite Surveying*, 4th Edition, Wiley, New York, 2015.
2. Rao, B. R., W. Kunysz, P. Fante, and K. McDonald, *GPS/GNSS Antennas*, Artech House, Norwood, 2013.
3. Counselman, C. C., "Multipath-rejecting GPS antennas," *Proceedings of the IEEE*, Vol. 87, No. 1, 86–91, 1999.
4. Lopez, A. R., "GPS landing system reference antenna," *IEEE Antennas and Propagation Magazine*, Vol. 52, No. 1, 105–113, 2010.
5. Tatarnikov, D. and A. Astakhov, "Large impedance ground plane antennas for mm-accuracy of gnss positioning in real time," *PIERS Proceedings*, 1825–1829, Stockholm, Sweden, 2013.
6. Attiya, A. M., "Omni-directional leaky-wave coaxial antenna," *PIERS Proceedings*, 1830–1833, Stockholm, Sweden, Aug. 12–15, 2013.
7. Tretyakov, S., *Analytical Modeling in Applied Electromagnetics*, Artech House, Norwood, 2003.
8. Tatarnikov, D., "Semi-transparent ground planes excited by magnetic line current," *IEEE Trans. Antennas and Propagation*, Vol. 60, No. 6, 2843–2852, 2012.